no longer be satisfied with *any* program that does the job, but only with those that will give us what we need at an acceptable cost. Most programs in our specialty have been written by engineers, rather than by programmers, out of necessity. It is understandable that, not having as much expertise in software as in microwave technology, the engineers produced programs that were not the most efficient ones, neither in the usage of storage nor in the utilization of central processor time.

The time has come for us to recognize that we can reduce the cost of our CAD's by seeking help from those among us who have more than a casual knowledge of Basic or Fortran. As there are engineers specializing in instrumentation who build our measurement gear or those specializing in devices who build our components, so in the coming years there will emerge engineers who will interface with the computer world. They will write our CAD programs and will be the custodians of our computer-backed hardware. These specialists will exchange information within our own technical environment (including, it is hoped, over the pages of S-MTT TRANSACTIONS) about hardware and software techniques that produce good design aids, and we shall have to create standards of performance by which these tools can be objectively evaluated.

Semiconductor Device Simulation

CHARLES M. LEE, RONALD J. LOMAX, SENIOR MEMBER, IEEE, AND GEORGE I. HADDAD, FELLOW, IEEE

(*Invited Paper*)

***Abstract*—Two of the numerical methods most widely used in solving the set of partial differential transport equations for holes, electrons, and electric field in semiconductor devices and the various numerical instability phenomena which can be encountered are described in detail. Also presented are approaches, using these methods, to calculate dc static solutions and small-signal solutions, and to simulate devices in voltage-driven, current-driven, and circuit-loaded operation. Sample results are given for each mode of operation for the case of Si avalanche-diode oscillators. The numerical methods and approaches are those developed at our laboratory and sufficient detail is presented to permit the development of similar Fortran codes by others.**

INTRODUCTION

THE DEVELOPMENT of semiconductor devices with complex modes of operation, such as avalanche diodes, has necessitated the development of detailed analysis for the behavior of holes and electrons and their interaction with electric fields in such devices. However, the nonlinearity of the equations which describe the behavior of these particles in high electric fields, particularly when space charge is significant or at high-frequency operation, imposes severe restrictions upon any attempt to obtain analytical closed-form solutions. Because of the collision-dominated conduction process, the particle trajectory methods developed extensively to study plasma phenomena have little application to semiconductors. Hence, numerical simulations [1]-[38] of semiconductor devices have emerged as powerful tools for their study. In this paper, some of these numerical methods, and in particular those that have been developed and used by the authors for simulating semiconductor devices and determining their operating characteristics, are presented and reviewed.

Manuscript received October 10, 1973; revised November 21, 1973. This work was supported by the Air Force Systems Command, Rome Air Development Center, under Contract F30602-71-C-0099.

C. M. Lee was with the Electron Physics Laboratory, Department of Electrical and Computer Engineering, University of Michigan, Ann Arbor, Mich. 48104. He is now with Bell Laboratories, Murray Hill, N. J. 08540.

R. J. Lomax and G. I. Haddad are with the Electron Physics Laboratory, Department of Electrical and Computer Engineering, University of Michigan, Ann Arbor, Mich. 48104.

THE TRANSPORT EQUATIONS

The behavior of holes and electrons in a one-dimensional model of a semiconductor can be characterized by the following partial differential equations:[1] the continuity equation for holes:

$$\frac{\partial P}{\partial t} + \frac{\partial JP}{\partial x} - G = 0 \tag{1}$$

the continuity equation for electrons:

$$\frac{\partial N}{\partial t} - \frac{\partial JN}{\partial x} - G = 0 \tag{2}$$

and Poisson's equation:

$$\frac{\partial E}{\partial x} - \frac{q}{\epsilon}(P - N - N_D) = 0 \tag{3}$$

where

[1] The notation in this paper is chosen for easy translation into a computer language (specifically Fortran).

$$JP = UP \cdot E \cdot P - \frac{kT}{q} \cdot UP \cdot \frac{\partial P}{\partial x} \tag{4}$$

$$JN = UN \cdot E \cdot N + \frac{kT}{q} \cdot UN \cdot \frac{\partial N}{\partial x} \tag{5}$$

$$G = IP \cdot |JP| + IN \cdot |JN| - \frac{P \cdot N - n_i^2}{\tau_r(P + N + 2n_i)} \tag{6}$$

t time (s);
x distance (cm);
P hole density (cm^{-3});
N electron density (cm^{-3});
JP hole particle current density ($cm^{-2} \cdot s^{-1}$);
JN electron particle current density ($cm^{-2} \cdot s^{-1}$);
G impact and thermal generation rate ($cm^{-3} \cdot s^{-1}$);
E electric-field intensity ($V \cdot cm^{-1}$);
q electronic charge (C);
ϵ dielectric constant ($F \cdot cm^{-1}$);
N_D doping density (cm^{-3}) (positive for the p-type dopant, negative for the n-type dopant);
UP hole mobility ($cm^2 \cdot V^{-1} \cdot s^{-1}$);
UN electron mobility ($cm^2 \cdot V^{-1} \cdot s^{-1}$);
k Boltzmann constant (J/K);
T absolute temperature (K);
IP hole ionization coefficient (cm^{-1});
IN electron ionization coefficient (cm^{-1});
τ_r carrier lifetime (s);
n_i intrinsic particle density (cm^{-3}).

The material parameters UP, UN, IP, and IN are functions of electric-field intensity. These may be functionally approximated but for greater accuracy and computation speed are usually stored in files in tabular form based on measured data and extrapolations of measured data. Intermediate values are linearly interpolated. To solve the preceding set of nonlinear partial differential equations on a digital computer, they are approximated by a set of difference equations. These difference equations are solved for a given set of initial conditions and boundary conditions. The various numerical methods differ in how these difference equations are derived and solved. In this paper, two numerical methods will be discussed.

The Explicit Method

In this numerical method, a time–space mesh shown in Fig. 1 is chosen to derive the difference equations. Namely, the one-dimensional semiconductor is divided into JW partitions. At both ends of each partition there are space-charge points J ($J = 1,\cdots,JW + 1$), and the hole density, electron density, and doping density are defined at these space-charge points. In the middle of the two space-charge points, there are field points I ($I = 1,\cdots,JW$) and the electric-field intensity, hole current density, and electron current density and those material parameters which are functions of the electric-field intensity are defined at these field points. The upstream particle density

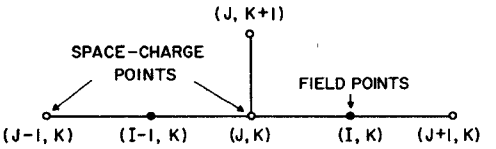

Fig. 1. Time–space mesh for the explicit method ($x = J \cdot \Delta x$, $J = 1,\cdots,JW + 1$; $t = K \cdot \Delta t$, $K = 1,\cdots,KP$).

is used in the drift current density terms and a central difference is used in the diffusion current density terms. In the explicit method, forward time differences are used. The difference equations for the particle current densities are, for $E_I^K \geq 0$,

$$JP_I^K = UP_I^K \cdot E_I^K \cdot P_J^K - \frac{kT}{q} \cdot UP_I^K \cdot (P_{J+1}^K - P_J^K)/\Delta x \tag{7}$$

and

$$JN_I^K = UN_I^K \cdot E_I^K \cdot N_{J+1}^K + \frac{kT}{q} \cdot UN_I^K \cdot (N_{J+1}^K - N_J^K)/\Delta x \tag{8}$$

for $E_I^K < 0$,

$$JP_I^K = UP_I^K \cdot E_I^K \cdot P_{J+1}^K - \frac{kT}{q} \cdot UP_I^K \cdot (P_{J+1}^K - P_J^K)/\Delta x \tag{9}$$

and

$$JN_I^K = UN_I^K \cdot E_I^K \cdot N_J^K + \frac{kT}{q} \cdot UN_I^K \cdot (N_{J+1}^K - N_J^K)/\Delta x. \tag{10}$$

The generation terms at the I points and the J points are approximated by

$$G_I^K = IP_I^K \cdot |JP_I^K| + IN_I^K \cdot |JN_I^K| \tag{11}$$

and

$$G_J^K = \tfrac{1}{2}(G_I^K + G_{I-1}^K) + \frac{P_J^K \cdot N_J^K - n_i^2}{\tau_r(P_J^K + N_J^K + 2n_i)}. \tag{12}$$

Given the preceding expressions, the continuity equations for holes and electrons and Poisson's equation can be rewritten as

$$P_J^{K+1} = P_J^K + \Delta t \cdot [G_J^K - (JP_I^K - JP_{I-1}^K)/\Delta x] \tag{13}$$

$$N_J^{K+1} = N_J^K + \Delta t \cdot [G_J^K + (JN_I^K - JN_{I-1}^K)/\Delta x] \tag{14}$$

and

$$E_I^{K+1} = E_{I-1}^{K+1} + \frac{q}{\epsilon}(P_J^{K+1} - N_J^{K+1} - N_{DJ})\Delta x. \tag{15}$$

For a given solution vector P_J^K, N_J^K ($J = 2,\cdots,JW$) and E_I^K ($I = 1,\cdots,JW$) at the Kth time step, the values of UP_I^K, UN_I^K, IP_I^K, and IN_I^K are obtained by linear

interpolations of the mobility tables and ionization tables. Then the particle current densities JP_I^K and JN_I^K are calculated from (7) through (10) and the generation terms G_I^K and G_J^K are calculated from (11) and (12). Based on the preceding information at the Kth time step, (13) and (14) are used to calculate the particle densities P_J^{K+1} and N_J^{K+1} ($J = 2,\cdots,JW$) at the $(K+1)$th time step. The values of P_1^{K+1}, N_1^{K+1}, P_{JW+1}^{K+1}, and N_{JW+1}^{K+1} are given by properly chosen space-charge boundary conditions at the assumed metal–semiconductor interfaces. The electric-field intensities E_I^{K+1} ($I = 1,\cdots,JW$) are calculated from (15) with the value of E_1^{K+1} chosen to satisfy a proper electric-field boundary condition. At this point, the advancement of the solution from the Kth time step to the $(K+1)$th time step is finished. This procedure can be repeated to advance the solution to $K+2$, $K+3,\cdots$, etc.

For each time advancement, the time step Δt is not a constant. In fact, the value of Δt has to be determined at each time step to satisfy certain numerical stability conditions in order to ensure that the numerical model does not result in oscillatory behavior and diverge. There are three stability conditions of this sort that have to be observed as follows.

1) Causality Stability Condition: The effect (or the response) of an excitation (or the state of the solution) at the Kth time step will propagate to the $(K+1)$th time step in the time–space domain following a certain characteristic path which can be interpreted as a causality relation between the excitation and the response. If the time step Δt in the time–space mesh is chosen too large, it will result, in effect, in a calculation of the response from insufficient information about the excitation and a numerical instability will occur. The instability usually occurs when the electric-field intensity is high and particles move at the saturated velocity. This instability is associated with the $\partial JP/\partial x$ and $\partial JN/\partial x$ terms in the continuity equations. If only these two terms are retained in (13) and (14), then substituting $VP_{\max}$ and $VN_{\max}$ (the maximum values of the particle drift velocities VP and VN) for VP and VN and $DP_{\max}$ and $DN_{\max}$ (the maximum values of the particle diffusion constants DP and DN) for DP and DN yields

$$\begin{aligned}(P_J^{K+1} - P_J^K)/\Delta t &= -\{[VP_{\max}\cdot P_J^K - DP_{\max}(P_{J+1}^K - P_J^K)/\Delta x] \\ &\quad - [VP_{\max}\cdot P_{J-1}^K - DP_{\max}\cdot(P_J^K - P_{J-1}^K)/\Delta x]\}/\Delta x\end{aligned} \tag{16}$$

and

$$\begin{aligned}(N_J^{K+1} - N_J^K)/\Delta t &= \{[VN_{\max}\cdot N_{J+1}^K + DN_{\max}\cdot(N_{J+1}^K - N_J^K)/\Delta x] \\ &\quad - [VN_{\max}\cdot N_J^K + DN_{\max} \\ &\quad \cdot(N_J^K - N_{J-1}^K)/\Delta x]\}/\Delta x.\end{aligned} \tag{17}$$

If P_J^K and N_J^K are smooth enough to be represented as

$$P_J^K = \sum_{m=-\infty}^{\infty} P_m \exp(imJ\Delta x)\cdot(g_{p,m})^K \tag{18}$$

and

$$N_J^K = \sum_{m=-\infty}^{\infty} N_m \exp(imJ\Delta x)\cdot(g_{n,m})^K \tag{19}$$

the growth factors $g_{p,m}$ and $g_{n,m}$ can be expressed as

$$g_{p,m} = (1 - A_p) + A_p\cos(m\cdot\Delta x) - iB_p\sin(m\cdot\Delta x) \tag{20}$$

and

$$g_{n,m} = (1 - A_n) + A_n\cos(m\cdot\Delta x) + iB_n\sin(m\cdot\Delta x) \tag{21}$$

where

$$A_p = \frac{2DP_{\max}\cdot\Delta t}{\Delta x^2} + \frac{VP_{\max}\cdot\Delta t}{\Delta x} \tag{22}$$

$$B_p = \frac{VP_{\max}\cdot\Delta t}{\Delta x} \tag{23}$$

$$A_n = \frac{2DN_{\max}\cdot\Delta t}{\Delta x^2} + \frac{VN_{\max}\cdot\Delta t}{\Delta x} \tag{24}$$

and

$$B_n = \frac{VN_{\max}\cdot\Delta t}{\Delta x}. \tag{25}$$

In the complex plane $g_{p,m}$ and $g_{n,m}$ generate two ellipses centered at $(1 - A_p)$ and $(1 - A_n)$ with major axes of $2A_p$ and $2A_n$ and minor axes of $2B_p$ and $2B_n$, respectively. These are shown in Fig. 2. To maintain numerical stability, the absolute values of $g_{p,m}$ and $g_{n,m}$ must be kept less than unity, i.e.,

$$|g_{p,m}| \le 1 \quad \text{and} \quad |g_{n,m}| \le 1 \tag{26}$$

for all m. This requires that $|A_p| \le 1$ and $|A_n| \le 1$. Let $V_{\max}$ be the larger of $VP_{\max}$ and $VN_{\max}$ and $D_{\max}$ be the larger of $DP_{\max}$ and $DN_{\max}$, then the time step Δt must be chosen such that

$$\Delta t \le \frac{\Delta x^2}{2\cdot D_{\max} + V_{\max}\cdot\Delta x}. \tag{27}$$

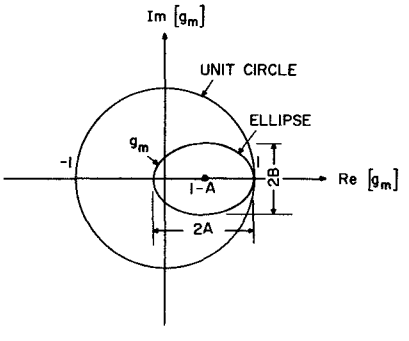

Fig. 2. The growth factor in the complex plane.

If this stability condition is violated, the values of the particle densities will oscillate around a zero level at a frequency of $1/(2\cdot\Delta t)$.

2) Space-Charge Stability Condition: This instability usually occurs when the electric field is low, the particle densities are high, and the space charge is almost neutral and uniform. In this case, the most important terms in the continuity equations are

$$\frac{\partial P}{\partial t} = -P\frac{\partial VP}{\partial x} \tag{28}$$

and

$$\frac{\partial N}{\partial t} = N\frac{\partial VN}{\partial x} \tag{29}$$

and Poisson's equation is

$$\frac{\partial E}{\partial x} = \frac{q}{\epsilon}\cdot\Delta Q \tag{30}$$

where ΔQ is the net space-charge particle density. Since

$$\frac{\partial VP}{\partial x} = \frac{\partial VP}{\partial E}\cdot\frac{\partial E}{\partial x} = \frac{q\cdot UP'}{\epsilon}\cdot\Delta Q \tag{31}$$

and

$$\frac{\partial VN}{\partial x} = \frac{\partial VN}{\partial E}\cdot\frac{\partial E}{\partial x} = \frac{q\cdot UN'}{\epsilon}\cdot\Delta Q \tag{32}$$

where UP' and UN' are the dynamic mobilities, the continuity equations become

$$\frac{\partial \Delta Q}{\partial t} = -\frac{1}{\tau'}\Delta Q \tag{33}$$

where τ' is the dynamic dielectric relaxation time constant

$$\frac{1}{\tau'} = \frac{1}{\tau_p'} + \frac{1}{\tau_n'} \tag{34}$$

$$\frac{1}{\tau_p'} = \frac{q\cdot P\cdot UP'}{\epsilon} \tag{35}$$

and

$$\frac{1}{\tau_n'} = \frac{q\cdot N\cdot UN'}{\epsilon}. \tag{36}$$

Equation (33) signifies that if there were any charge imbalance ΔQ it would relax exponentially to neutrality with a time constant which is the local dynamic dielectric relaxation time constant τ'. However, in solving these difference equations it is assumed that the rate of change of ΔQ is constant over the time interval Δt, hence, the change of ΔQ versus time follows the tangent line of the exponential curve. If $\Delta t > 2\,|\,\tau'\,|$, the value of ΔQ will overshoot to the opposite side of neutrality and result in an even larger charge imbalance of the opposite sign at the next time step. This phenomenon will be repeated for each successive time step and the net space charge will oscillate and increase indefinitely. To avoid this instability, the time step for each instant of time must be chosen to satisfy the following space-charge stability condition:

$$\Delta t < 2\cdot|\,\tau'\,|. \tag{37}$$

3) Field Stability Condition: This instability usually occurs at a location where there is a large gradient of particle density, such as at the transition between lightly doped and heavily doped regions. Because of the large gradient, the relative movement of particles will result in a change in the net space charge of

$$\Delta Q = q(\Delta JP + \Delta JN)\cdot\Delta t.$$

This change in space charge will modify the electric field by $\Delta E = q\cdot\Delta Q/\epsilon$, and the modification of the electric field will affect the movement of particles after a time delay of Δt. Since

$$JP + JN = UP\cdot E\cdot P - DP\cdot\frac{\partial P}{\partial x} + UN\cdot E\cdot N + DN\frac{\partial N}{\partial x} \tag{38}$$

and if E_0 is the electric-field intensity which would yield zero particle current for a given calculated particle density profile, i.e.,

$$E_0 = \frac{1}{UP\cdot P + UN\cdot N}\cdot\left(DP\frac{\partial P}{\partial x} - DN\frac{\partial N}{\partial x}\right) \tag{39}$$

then

$$JP + JN = (UP\cdot P + UN\cdot N)\cdot(E - E_0). \tag{40}$$

Therefore, the loop gain of the preceding interaction is

$$\left|\frac{\Delta Q}{\Delta(JP+JN)}\right|\cdot\left|\frac{\Delta E}{\Delta Q}\right|\cdot\left|\frac{\Delta(JP+JN)}{\Delta E}\right| = \frac{q\cdot(UP\cdot P + UN\cdot N)}{\epsilon}\cdot\Delta t = \Delta t/\tau \tag{41}$$

where τ is the local static dielectric relaxation time constant and is given by

$$\frac{1}{\tau} = \frac{1}{\tau_p} + \frac{1}{\tau_n}$$

where

$$\frac{1}{\tau_p} = \frac{q\cdot UP\cdot P}{\epsilon}$$

and

$$\frac{1}{\tau_n} = \frac{q\cdot UN\cdot N}{\epsilon}.$$

If $\Delta t > 2\cdot\tau$, the change in the net space charge accumulated during this time interval will be so large as to make the value of E overshoot to less than E_0 and cause a particle current flow in the opposite direction at the next time step. If this process is repeated for each time step, the particles appear to move alternately to the left and

to the right and the electric field oscillates around the E_0 level. Hence, Δt must be chosen to satisfy the field stability condition

$$\Delta t < 2 \cdot | \tau | .$$

Although both the space-charge instability and the field instability involve the effect of net space charge, in the first instability the change of the net space charge is caused by the gradient of the electric field while in the second instability the change of the net space charge is caused by the gradient of the particle density. Also, if the thermal recombination lifetime τ_r is very short, there will be an instability related to it, and the stability condition (37) must be modified to include the term $1/\tau_r$. However, in most situations τ_r is too long to be important.

It is important to stress that the preceding stability criteria should not be considered rigorous in any mathematical sense. The justification for these criteria lies in the personal experience that in the numerous computer runs made, when these stability conditions were met, no instability was observed.

The Implicit Method[2]

In this numerical method, the time–space mesh as shown in Fig. 3 is chosen in deriving the difference equations. Let the vector $[Q]$ and the vector $[F]$ be defined by

$$[Q] = \begin{bmatrix} P \\ \\ N \end{bmatrix} \qquad [F] = \begin{bmatrix} FP \\ \\ FN \end{bmatrix} = \begin{bmatrix} G - (\partial JP/\partial x) \\ \\ G + (\partial JN/\partial x) \end{bmatrix}. \tag{42}$$

The definitions of JP, JN, and G are the same as in the explicit method except the recombination term is ignored. The objective is to find a difference equation to approximate the continuity equations evaluated at the instant of time halfway between the Kth time step and the $(K + 1)$th time step, or

$$\left[\frac{\partial Q}{\partial t}\right]^{K+(1/2)} = [F]^{K+(1/2)}. \tag{43}$$

Since $[F]$ is a nonlinear function of the solution and the solution at $K + (1/2)$ is unknown, the procedure is to expand the $[F]$ vector in terms of the solution at the Kth time step

$$\left[\frac{\Delta Q}{\Delta t}\right]^{K+(1/2)} = [F]^K + \frac{\partial}{\partial Q}[F]^K \cdot \left[\frac{\Delta Q}{2}\right] + \frac{\partial}{\partial E}[F]^K \cdot \left[\frac{\Delta E}{2}\right]. \tag{44}$$

Rearranging the terms yields

$$\left[\frac{2}{\Delta t} - \frac{\partial}{\partial Q}[F]^K\right] \cdot [\Delta Q] - \frac{\partial}{\partial E}[F]^K \cdot [\Delta E] = 2[F]^K. \tag{45}$$

This equation is identical to Scharfetter and Gummel's [11] difference equation, although the argument used in its derivation is slightly different. Let the space-charge operator be defined as

$$[ZQ]^K = \left[\frac{2}{\Delta t} - \frac{\partial}{\partial Q}[F]^K\right] \tag{46}$$

the field operator as

$$[ZE]^K = \left[-\frac{\partial}{\partial E}[F]^K\right] \tag{47}$$

and the force vector as

$$[ZF]^K = 2[F]^K. \tag{48}$$

Then (45) becomes

$$[ZQ]^K \cdot [\Delta Q]^K + [ZE]^K \cdot [\Delta E]^K = [ZF]^K. \tag{49}$$

Equation (49) can be rewritten in more detail as

$$\begin{bmatrix} [ZQ_{2,2}][ZQ_{2,3}] & & & & \\ [ZQ_{3,2}][ZQ_{3,3}][ZQ_{3,4}] & & & & \\ & \ddots & & & \\ & [ZQ_{J,J-1}][ZQ_{J,J}][ZQ_{J,J+1}] & & & \\ & & \ddots & & \\ & & [ZQ_{JW-1,JW-2}][ZQ_{JW-1,JW-1}][ZQ_{JW-1,JW}] & & \\ & & & [ZQ_{JW,JW-1}] & [ZQ_{JW,JW}] \end{bmatrix}^K \cdot \begin{bmatrix} \Delta P_2 \\ \Delta N_2 \\ \vdots \\ \Delta P_J \\ \Delta N_J \\ \vdots \\ \Delta P_{JW} \\ \Delta N_{JW} \end{bmatrix}^K$$

$$+ \begin{bmatrix} [ZE_{2,1}][ZE_{2,2}] & & & & \\ & [ZE_{3,2}][ZE_{3,3}] & & & \\ & & \ddots & & \\ & & & [ZE_{I,I-1}][ZE_{I,I}] & \\ & & & & \ddots \\ & & & & [ZE_{JW,JW-1}][ZE_{JW,JW}] \end{bmatrix}^K \cdot \begin{bmatrix} \Delta E_1 \\ \vdots \\ \Delta E_I \\ \vdots \\ \Delta E_{JW} \end{bmatrix}^K = \begin{bmatrix} 2F_2 \\ \vdots \\ 2F_J \\ \vdots \\ 2F_{JW} \end{bmatrix}^K \tag{50}$$

where

[2] This is based on Scharfetter and Gummel's [11] method, except for a modification in the boundary conditions.

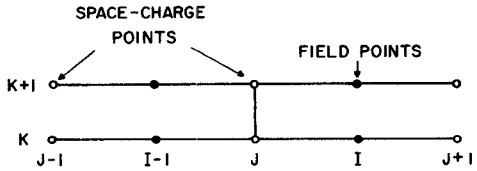

Fig. 3. Time–space mesh for the implicit method ($x = J \cdot \Delta x$, $J = 1,\cdots,JW + 1$; $t = K \cdot \Delta t$, $K = 1,\cdots,KP$).

$$[ZQ_{J,J-1}][ZQ_{J,J}][ZQ_{J,J+1}] = \left[\begin{bmatrix} -\frac{\partial FP_J}{\partial P_{J-1}}, -\frac{\partial FP_J}{\partial N_{J-1}} \\ -\frac{\partial FN_J}{\partial P_{J-1}}, -\frac{\partial FN_J}{\partial N_{J-1}} \end{bmatrix}, \begin{bmatrix} \frac{2}{\Delta t} - \frac{\partial FP_J}{\partial P_J}, -\frac{\partial FP_J}{\partial N_J} \\ -\frac{\partial FN_J}{\partial P_J}, \frac{2}{\Delta t} - \frac{\partial FN_J}{\partial N_J} \end{bmatrix}, \begin{bmatrix} -\frac{\partial FP_J}{\partial P_{J+1}}, -\frac{\partial FP_J}{\partial N_{J+1}} \\ -\frac{\partial FN_J}{\partial P_{J+1}}, -\frac{\partial FN_J}{\partial N_{J+1}} \end{bmatrix}\right] \quad (51)$$

and

$$[ZE_{J,I-1}][ZE_{J,I}] = \left[\begin{bmatrix} -\frac{\partial FP_J}{\partial E_{I-1}} \\ -\frac{\partial FN_J}{\partial E_{I-1}} \end{bmatrix}, \begin{bmatrix} -\frac{\partial FP_J}{\partial E_I} \\ -\frac{\partial FN_J}{\partial E_I} \end{bmatrix}\right]. \quad (52)$$

In (50) the large matrices are block tridiagonal and tridiagonal, respectively, other terms being zero. The terms in these matrices are calculated at each time step (see the Appendix). Thus at each J point

$$[ZQ_{J,J-1}, ZQ_{J,J}, ZQ_{J,J+1}] \cdot \begin{bmatrix} \Delta Q_{J-1} \\ \Delta Q_J \\ \Delta Q_{J+1} \end{bmatrix} + [ZE_{J,I-1}, ZE_{J,I}] \cdot \begin{bmatrix} \Delta E_{I-1} \\ \Delta E_I \end{bmatrix} = [ZF_J]. \quad (53)$$

Poisson's equation can be used to reduce this $[Z]$ matrix equation to a $[T]$ matrix equation (defined later). Define $QDXOEP$ by the following:

$$QDXOEP = q \cdot \Delta x/\epsilon$$

then Poisson's equation is

$$\Delta E_{I-1} = \Delta E_I - QDXOEP \cdot (\Delta P_J - \Delta N_J). \quad (54)$$

This can be used in the $[Z]$ matrix equation to obtain the $[T]$ matrix equation:

$$[TQ_{J,J-1}, TQ_{J,J}, TQ_{J,J+1}] \cdot \begin{bmatrix} \Delta Q_{J-1} \\ \Delta Q_J \\ \Delta Q_{J+1} \end{bmatrix} + [TE_{J,I}] \cdot [\Delta E_I] = [TF_J] \quad (55)$$

where

$$[TQ_{J,J-1}] = [ZQ_{J,J-1}] \quad (56)$$

$$[TQ_{J,J}] = [ZQ_{J,J}] - QDXOEP \cdot [ZE_{J,I-1} - ZE_{J,I-1}] \quad (57)$$

$$[TQ_{J,J+1}] = [ZQ_{J,J+1}] \quad (58)$$

$$[TE_{J,I}] = [ZE_{J,I-1}] + [ZE_{J,I}] \quad (59)$$

and

$$[TF_J] = [ZF_J]. \quad (60)$$

The preceding $[T]$ matrix equation can be further reduced to an $[S]$ matrix equation by assuming that the following recursion relation exists:

$$[\Delta Q_J] = [QF_J] + [QQ_{J,J+1}] \cdot [\Delta Q_{J+1}] + [QE_{J,I}][\Delta E_I] \quad (61)$$

or

$$[\Delta Q_{J-1}] = [QF_{J-1}] + [QQ_{J-1,J}] \cdot [\Delta Q_J] + [QE_{J-1,I-1}][\Delta E_{I-1}]. \quad (62)$$

Multiplying by $[TQ_{J,J-1}]$ on both sides of the preceding equation gives

$$[TQ_{J,J-1}] \cdot [\Delta Q_{J-1}] - [TQ_{J,J-1}][QQ_{J-1,J}][\Delta Q_J] - [TQ_{J,J-1}] \cdot [QE_{J-1,I-1}][\Delta E_{I-1}] = [TQ_{J,J-1}][QF_{J-1}]. \quad (63)$$

Eliminating the $[\Delta Q_{J-1}]$ term in (63) by using (55) yields

$$([TQ_{J,J}] + [TQ_{J,J-1}][QQ_{J-1,J}]) \cdot [\Delta Q_J] + [TQ_{J,J+1}][\Delta Q_{J+1}] + [TE_{J,I}][\Delta E_I] + [TQ_{J,J-1}][QE_{J-1,I-1}][\Delta E_{I-1}] = [TF_J] - [TQ_{J,J-1}][QF_{J-1}]. \quad (64)$$

Using Poisson's equation again to eliminate the $[\Delta E_{I-1}]$ term in (64) gives

$$([TQ_{J,J}] + [TQ_{J,J-1}][QQ_{J-1,J}] - QDXOEP \cdot [TQ_{J,J-1}] \cdot [[QE_{J-1,I-1}], -[QE_{J-1,I-1}]])[\Delta Q_J] + [TQ_{J,J+1}][\Delta Q_{J+1}] + ([TE_{J,I}] + [TQ_{J,J-1}] \cdot [QE_{J-1,I-1}])[\Delta E_I] = [TF_J] - [TQ_{J,J-1}][QF_{J-1}] \quad (65)$$

or

$$[SQ_{J,J}][\Delta Q_J] + [SQ_{J,J+1}][\Delta Q_{J+1}] + [SE_{J,I}][\Delta E_I] = [SF_J] \quad (66)$$

where

$$[TQQQ_J] = [TQ_{J,J-1}][QQ_{J-1,J}] \quad (67)$$

$$[TQQE_J] = [TQ_{J,J-1}][QE_{J-1,I-1}] \quad (68)$$

$$[TQQF_J] = [TQ_{J,J-1}][QF_{J-1}] \quad (69)$$

$$[SQ_{J,J}] = [TQ_{J,J}] + [TQQQ_J] - QDXOEP([TQQE_J], -[TQQE_J]) \quad (70)$$

$$[SQ_{J,J+1}] = [TQ_{J,J+1}] \tag{71}$$

$$[SE_{J,I}] = [TE_{J,I}] + [TQQE_J] \tag{72}$$

and

$$[SF_J] = [TF_J] - [TQQF_J]. \tag{73}$$

Finally, the $[Q]$ matrix equation is calculated from the $[S]$ matrix equation:

$$[\Delta Q_J] = [QF_J] + [QQ_{J,J+1}][\Delta Q_{J+1}] + [QE_{J,I}][\Delta E_I] \tag{74}$$

where

$$[QQ_{J,J+1}] = -[SQ_{J,J}]^{-1} \cdot [SQ_{J,J+1}] \tag{75}$$

$$[QE_{J,I}] = -[SQ_{J,J}]^{-1}[SE_{J,I}] \tag{76}$$

and

$$[QF_J] = [SQ_{J,J}]^{-1}[SF_J]. \tag{77}$$

To initialize the recursive calculations of (67)–(69), the starting values for $[QQ_{1,2}]$, $[QE_{1,1}]$, and $[QF_1]$ can be found as shown below. Recall that the boundary condition requires that $[\Delta Q_1] \equiv 0$. Notice that $[\Delta Q_1] = [QF_1] + [QQ_{1,2}][\Delta Q_2] + [QE_{1,1}][\Delta E_1]$. In order to obtain $[\Delta Q_1] \equiv 0$ for any calculated $[\Delta Q_2]$ and $[\Delta E_1]$, the following relations must hold:

$$[QQ_{1,2}] \equiv 0 \tag{78}$$

$$[QE_{1,1}] \equiv 0 \tag{79}$$

and

$$[QF_1] \equiv 0. \tag{80}$$

These are used as starting values to calculate $[QQ_{J,J+1}]$, $[QE_{J,I}]$, and $[QF_J]$ for $J = 2,\cdots,JW$.

The values of $[\Delta Q_{JW+1}]$ and $[\Delta E_{JW}]$ are set by boundary conditions. The solutions $[\Delta Q_J]$ $(J = 2,\cdots,JW)$ and $[\Delta E_I](I = 1,\cdots,JW)$ and then obtained by back substitutions, i.e., by repeatedly using (54) and (74).

DC Solutions

Both the explicit and implicit methods can be used to calculate dc static solutions. To start with, an initial guess of P_J, N_J $(J = 1,\cdots,JW + 1)$ and E_J $(J = 1,\cdots,JW)$ must be made. Then, one of these two methods is used to carry out the calculation for a sufficient time until the difference between two successive calculations is less than a preset tolerance (say 0.1 percent). The final calculation is considered to be the dc static solution.

At the boundary, it is assumed that the surface-state density is high enough so that the surface recombination velocity is infinite, and the semiconductor is very extrinsic. Hence, the particle density at the boundary is

$$\text{the majority particle density} = |\text{ doping density }| \tag{81}$$

and

$$\text{the minority particle density} = n_i^2/|\text{ doping density }|. \tag{82}$$

This is the boundary condition for the particle densities.

For the boundary condition on the electric field, intuitively one might be tempted to apply a constant total current across the device. However, if the device exhibits some negative conductance and zero susceptance at a certain frequency and if the device happens to be short-circuit stable at this frequency, the calculation, with a constant total current as a boundary condition, will result in a relaxation-type oscillation instead of a dc static solution. Hence, it is better to choose the value of the electric field at the boundaries iteratively such that the space average of the particle current density over the active region of the device is equal to the specified dc bias current.

For the explicit method, this boundary condition can be applied either to E_1 or to E_{JW}. The integration of Poisson's equation is then carried out from this boundary to the other boundary. For the implicit method, this boundary condition is applied to ΔE_{JW}; only the back substitution is repeated for each choice of ΔE_{JW}. Fig. 4 shows the dc static solutions of an n^+–p-p^+ Si diode biased at four different values of dc current.

Small-Signal Solutions

Once the dc static solution of a device is obtained, its small-signal solution can be calculated by applying perturbation theory to the dc static solution. To derive the perturbation equations, the continuity equations for holes and electrons and Poisson's equation [(1)–(3) and definitions (42)] are employed.

Introducing small-signal perturbations ΔP, ΔN, and ΔE yields

$$\left.\begin{aligned} P &= P_0 + \Delta P \\ N &= N_0 + \Delta N \end{aligned}\right\} \quad \text{or} \quad [Q] = [Q_0] + [\Delta Q] \tag{83}$$

$$E = E_0 + \Delta E \tag{84}$$

$$JP = JP_0 + \frac{\partial JP_0}{\partial P}\cdot\Delta P + \frac{\partial JP_0}{\partial N}\cdot\Delta N + \frac{\partial JP_0}{\partial E}\cdot\Delta E \tag{85}$$

$$JN = JN_0 + \frac{\partial JN_0}{\partial P}\cdot\Delta P + \frac{\partial JN_0}{\partial N}\cdot\Delta N + \frac{\partial JN_0}{\partial E}\cdot\Delta E \tag{86}$$

and

$$G = G_0 + \frac{\partial G_0}{\partial P}\cdot\Delta P + \frac{\partial G_0}{\partial N}\cdot\Delta N + \frac{\partial G_0}{\partial E}\cdot\Delta E \tag{87}$$

where P_0, N_0, E_0, JP_0, JN_0, and G_0 are the dc solutions, i.e.,

$$\frac{\partial JP_0}{\partial x} - G_0 = 0 \qquad \frac{\partial P_0}{\partial t} = 0 \tag{88}$$

$$-\frac{\partial JN_0}{\partial x} - G = 0 \qquad \frac{\partial N_0}{\partial t} = 0 \tag{89}$$

and

$$\frac{\partial E_0}{\partial x} - \frac{q}{\epsilon}(P_0 - N_0 - N_D) = 0 \qquad \frac{\partial E_0}{\partial t} = 0. \tag{90}$$

Assuming these small-signal perturbations vary in time proportionally to $\exp(j\omega t)$, substituting (83)–(87) into

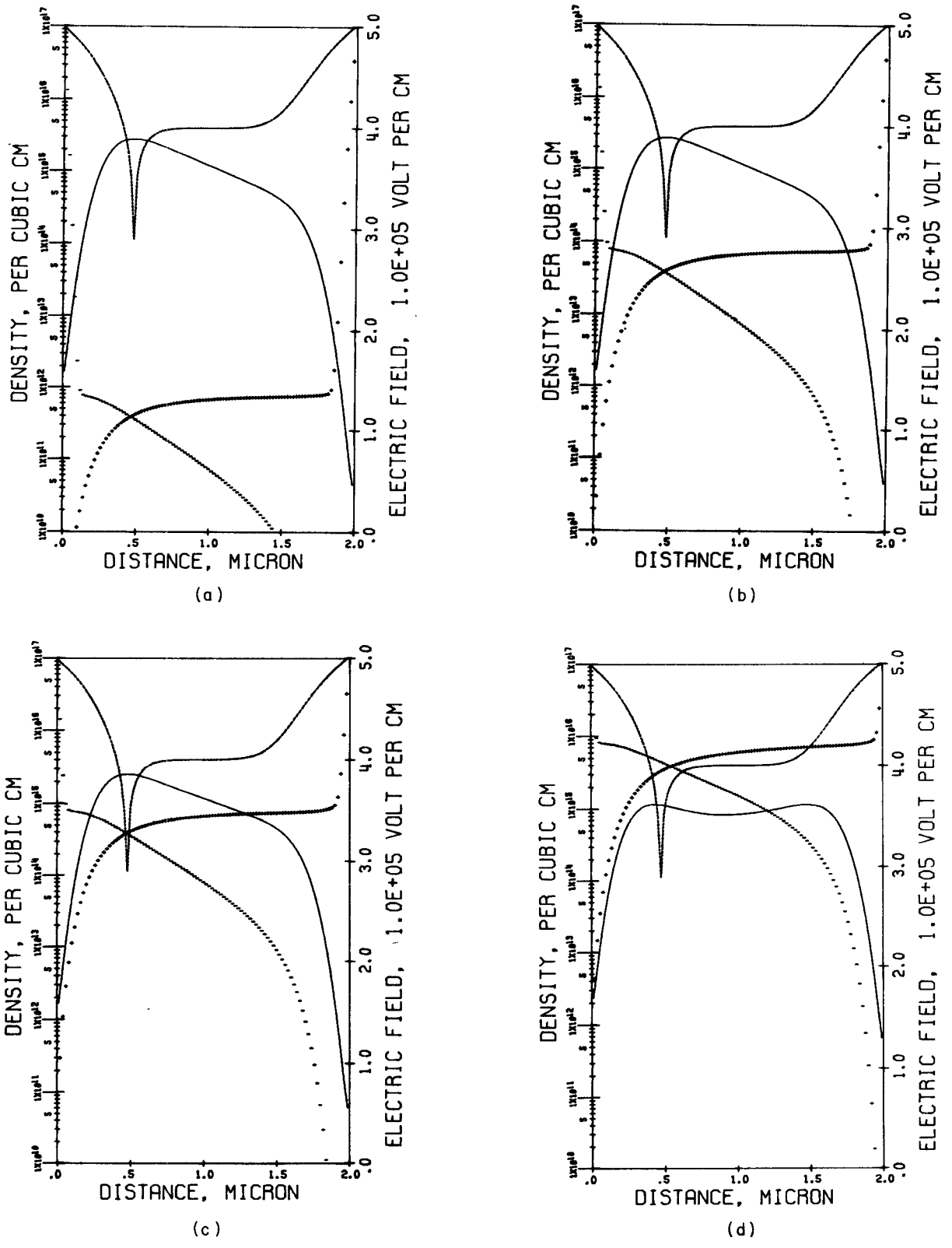

Fig. 4. The electric field (solid line), hole density (plus sign), electron density (minus sign), and doping density (dashed line) versus distance for an Si n^+-p-p^+ diode biased at different values of current density. (a) Silicon *P*-2-4-1 diode. *JDC* = 1.0 A/cm²; *VDC* = 64.22 V. (b) Silicon *P*-2-4-1 diode. *JDC* = 100.0 A/cm²; *VDC* = 64.35 V. (c) Silicon *P*-2-4-1 diode. *JDC* = 1.0 kA/cm²; *VDC* = 64.54 V. (d) Silicon *P*-2-4-1 diode. *JDC* = 10.0 kA/cm²; *VDC* = 66.09 V.

1)–(3) and eliminating all dc terms by using (88)–(90) ields

$$j\omega\Delta P = \frac{\partial FP}{\partial P}\Delta P + \frac{\partial FP}{\partial N}\Delta N + \frac{\partial FP}{\partial E}\Delta E \tag{91}$$

$$j\omega\Delta N = \frac{\partial FN}{\partial P}\Delta P + \frac{\partial FN}{\partial N}\Delta N + \frac{\partial FN}{\partial E}\Delta E \tag{92}$$

nd

$$\frac{\partial \Delta E}{\partial x} = \frac{q}{\epsilon}(\Delta P - \Delta N). \tag{93}$$

Equations (91) and (92) are rewritten in matrix form as ollows:

$$\left[j\omega - \frac{\partial}{\partial Q}[F]\right]\cdot[\Delta Q] - \frac{\partial}{\partial E}[F]\cdot[\Delta E] = [0]. \tag{94}$$

By using the same time–space mesh and the same formuations for JP_I^K, JN_I^K, and G_J^K that were used in the mplicit method, a system of matrix equations can be contructed similar to (50) and Poisson's equation with only he following differences.

1) Wherever $2/\Delta t$ occurred, $j\omega$ now appears.

2) Instead of $[2F^K]$ at the right-hand side of (50), the ull vector [0] now appears.

3) The doping density term is dropped in Poisson's quation.

4) All of the terms in the matrix equations are now omplex numbers or complex variables.

5) The ΔP, ΔN, and ΔE terms are redefined to be the erturbations instead of the changes of the solution during he time interval Δt.

Hence, after the dc static solution of a device biased t a specified dc current is obtained, the calculation of s small-signal solution at any specified frequency is imilar to one time-step advancement using the implicit ıethod. The implicit method computer program can be hanged into a small-signal program after some modificaions corresponding to the preceding differences.

The boundary conditions for the particle densities in he small-signal calculation are the same as those used in he implicit method.

The boundary condition for the electric field is derived s follows. Assume that the perturbation of the total urrent across the device is ΔJT. The continuity of total urrent at the point JW requires

$$JT = j\omega\epsilon\cdot\Delta E_{JW} + q\cdot(\Delta JP_{JW} + \Delta JN_{JW})$$

$$= j\omega\epsilon\cdot\Delta E_{JW} + q\cdot\left[\left(\frac{\partial JP}{\partial P}\right)_{JW}\Delta P_{JW} + \left(\frac{\partial JP}{\partial E}\right)_{JW}\cdot\Delta E_{JW} + \left(\frac{\partial JN}{\partial N}\right)_{JW}\cdot\Delta N_{JW} + \left(\frac{\partial JN}{\partial E}\right)_{JW}\cdot\Delta E_{JW}\right]$$

$$= \left[j\omega\epsilon + q\left(\frac{\partial JP}{\partial E}\right)_{JW} + q\left(\frac{\partial JN}{\partial E}\right)_{JW}\right]\cdot\Delta E_{JW} + \left[q\left(\frac{\partial JP}{\partial P}\right)_{JW}, q\left(\frac{\partial JN}{\partial N}\right)_{JW}\right]\begin{bmatrix}\Delta P_{JW}\\ \Delta N_{JW}\end{bmatrix}. \tag{95}$$

Since there is a null vector [0] at the right-hand side of the small-signal equation, i.e., $[ZF] \equiv 0$, it can be shown, when the $[Z]$ matrix equation is reduced into the $[Q]$ matrix equation, that always $[QF] = 0$. Recall $[\Delta Q]_{JW+1} \equiv 0$. Hence, at the JW point

$$\Delta Q_{JW} = QE_{JW,JW}\cdot\Delta E_{JW}$$

or

$$\begin{bmatrix}\Delta P_{JW}\\ \Delta N_{JW}\end{bmatrix} = \begin{bmatrix}QEP_{JW,JW}\\ QEN_{JW,JW}\end{bmatrix}\cdot\Delta E_{JW}. \tag{96}$$

Substituting (96) into (95) gives the following boundary condition for ΔE_{JW}:

$$\Delta E_{JW} = \frac{\Delta JT}{j\omega\epsilon + q[(\partial JP/\partial E)_{JW} + (\partial JN/\partial E)_{JW} + (\partial JP/\partial P)_{JW}\cdot QEP_{JW,JW} + (\partial JN/\partial N)_{JW}QEN_{JW,JW}]}. \tag{97}$$

Usually $\Delta JT = \exp(j\omega t)$ A/cm² is used in the calculation.

Once ΔP_J and ΔN_J $(J = 2,\cdots,JW)$ and ΔE_J $(J = 1,\cdots,JW)$ are calculated, the perturbation of the terminal voltage ΔVT can be found by

$$\Delta VT = \sum_{J=1}^{JW}(\Delta E_J\cdot\Delta x) \tag{98}$$

then the small-signal admittance and impedance can be calculated from ΔJT and ΔVT.

Fig. 5 shows the small-signal admittance of the same

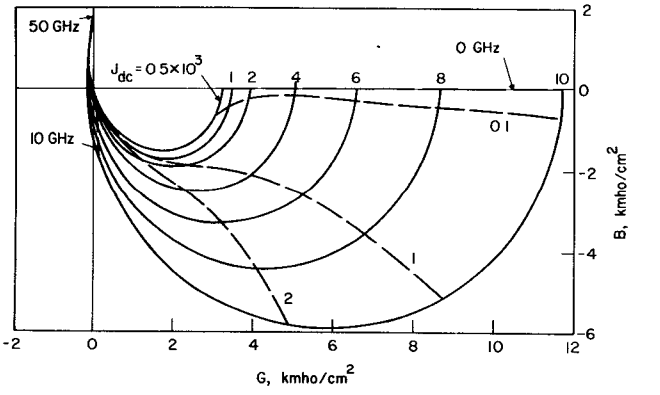

Fig. 5. Small-signal G-B locus of a 2-μm p-type Si diode for different bias currents.

n⁺-p-p⁺ Si diode biased at from 500 A/cm² up to 10 000 A/cm² dc current and over the frequency range from dc to 50 GHz.

The Simulation of Voltage-Driven RF Operations

The objective of this kind of simulation is to understand the device physics and to calculate the characteristics of the device either as an oscillator or as an amplifier when its terminal voltage is specified as a function of time.

The boundary conditions for the particle densities are the same as in the dc static calculation. The electric field at the boundary is chosen to yield the specified terminal voltage. For the explicit method, this is a one-shot calculation. For the implicit method, the value of $E_{JW}{}^{K}$ at each time step has to be chosen iteratively until this boundary condition is satisfied within a specified tolerance.

In some cases, it may be desired to study the RF operation of the device biased at a specified dc current density instead of a specified dc voltage. For this purpose, the circuit model shown in Fig. 6 can be used. Of course, the coupling network between the device and the RF voltage source can be made more complicated than the single capacitor shown in Fig. 6. The terminal voltage at each time step, which can be calculated by solving the circuit equation, is used as the boundary condition for the electric field.

Fig. 7 shows the terminal voltage waveform and induced current waveform versus time generated by using the explicit method for an n^+-p-p^+ Si diode biased with a dc current source of 1000 A/cm² and driven by a 25-GHz 10-V sinusoidal RF voltage, coupled through a 0.1-μF/cm² capacitor. However, this circuit model does not always yield single-frequency operation. When the device exhibits negative conductance at a low frequency and the coupling network is not chosen properly, this simulation sometimes results in some low-frequency bias circuit oscillation in addition to the specified RF voltage. Fig. 8 shows a sample of this lower frequency oscillation which occurs when the coupling capacitor in the simulation of Fig. 7 is changed to 0.01 μF/cm². To avoid these low-frequency oscillations, the simulation can be done in the following way. Assume the diode is driven by an RF voltage source and a dc voltage source connected in series. The frequency and amplitude of the RF voltage source have fixed values, but the dc voltage source is to be iteratively chosen to yield the desired dc bias current density at the end of each microwave period. The same solution vector for P, N, and E at zero phase angle is used repeatedly until the average current density over one microwave period is close enough to the specified J_{dc}, then the newly generated solution P, N, and E at 360° phase angle is used as the starting solution and the preceding iteration is repeated. The calculation is continued until the solution becomes periodic. The transient period of this simulation has no physical meaning because V_{dc} is constantly being adjusted artificially. However, it always yields a single-frequency RF voltage-driven periodic solution without the low-frequency bias circuit oscillation. Fig. 9 shows the terminal voltage and induced current waveform generated by this simulation method for the same n^+-p-p^+ Si diode driven by a 25-GHz 10-V RF voltage source and a dc voltage source to yield a dc bias current of 1000 A/cm². Fig. 10 shows the

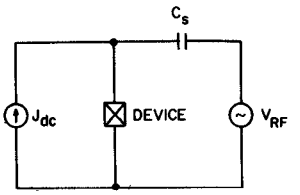

Fig. 6. Circuit model for the simulation of devices biased with specified dc current.

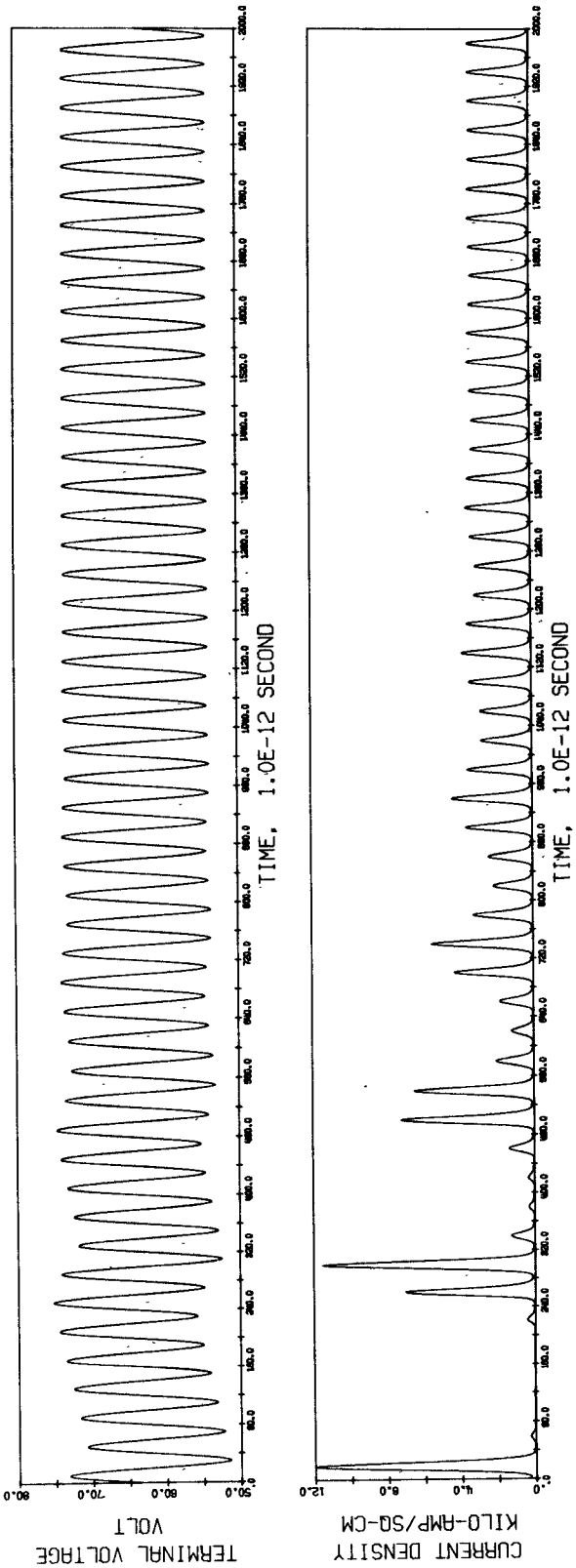

Fig. 7. Terminal voltage and particle current waveforms for the simulation of the IMPATT operation of an Si n^+-p-p^+ diode (J_{dc} = 1000 A/cm²; V_{RF} = 10 V; f = 25 GHz; C_s = 0.1 μF/cm²).

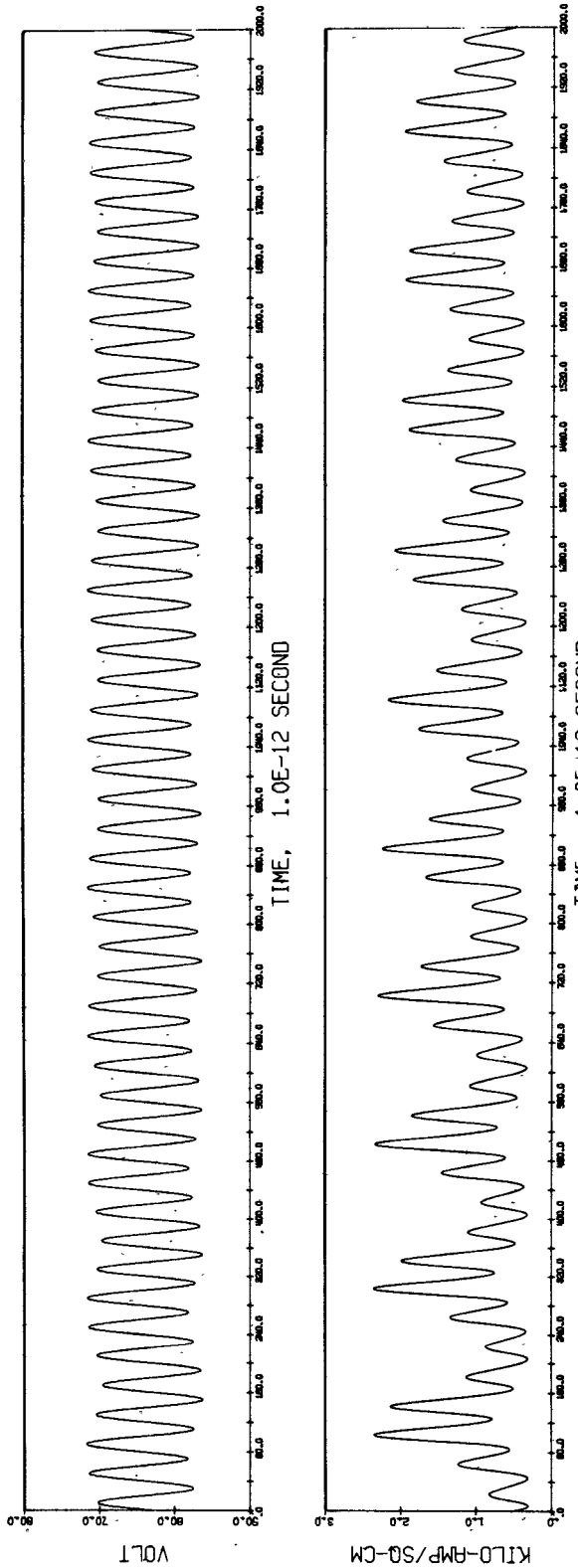

Fig. 8. Terminal voltage and particle current waveforms for the simulation of the IMPATT operation of an Si n^+-p-p^+ diode (J_{dc} = 1000 A/cm²; V_{RF} = 10 V; f = 25 GHz; C_s = 0.01 μF/cm²).

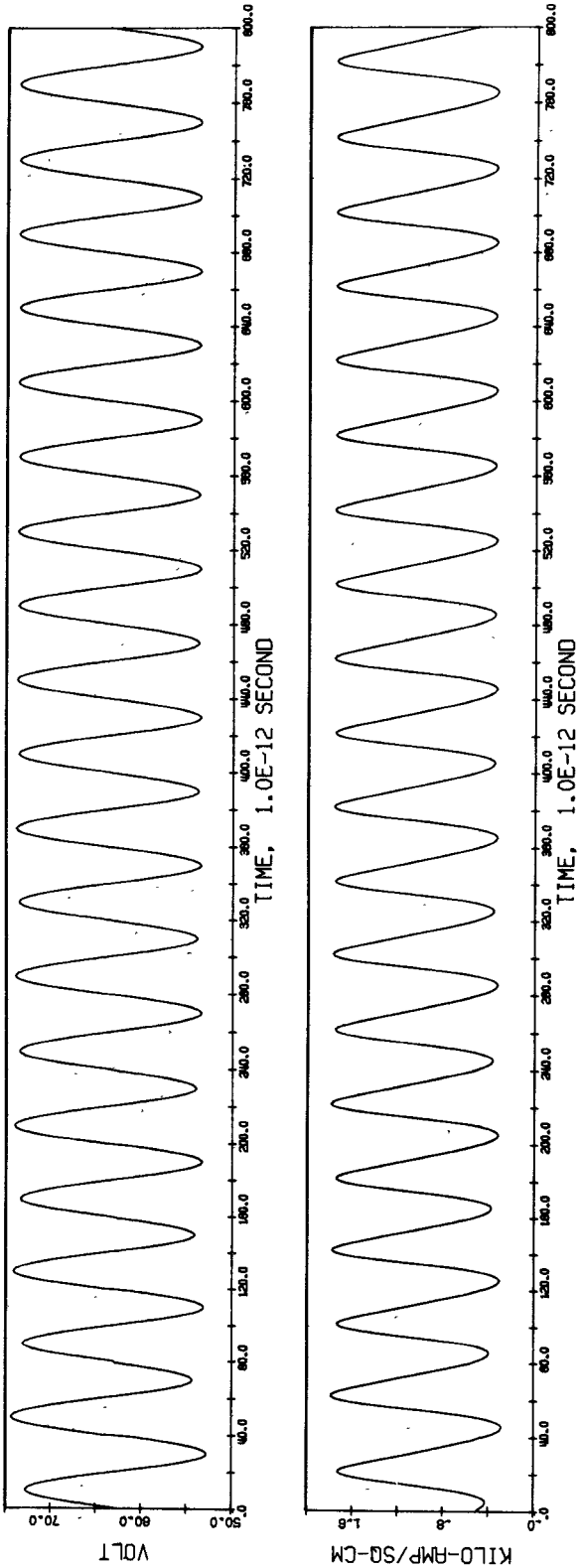

Fig. 9. Terminal voltage and particle current waveforms for the simulation of the IMPATT operation of an Si n^+-p-p^+ diode (J_{dc} = 1000 A/cm²; V_{RF} = 10 V; f = 25 GHz).

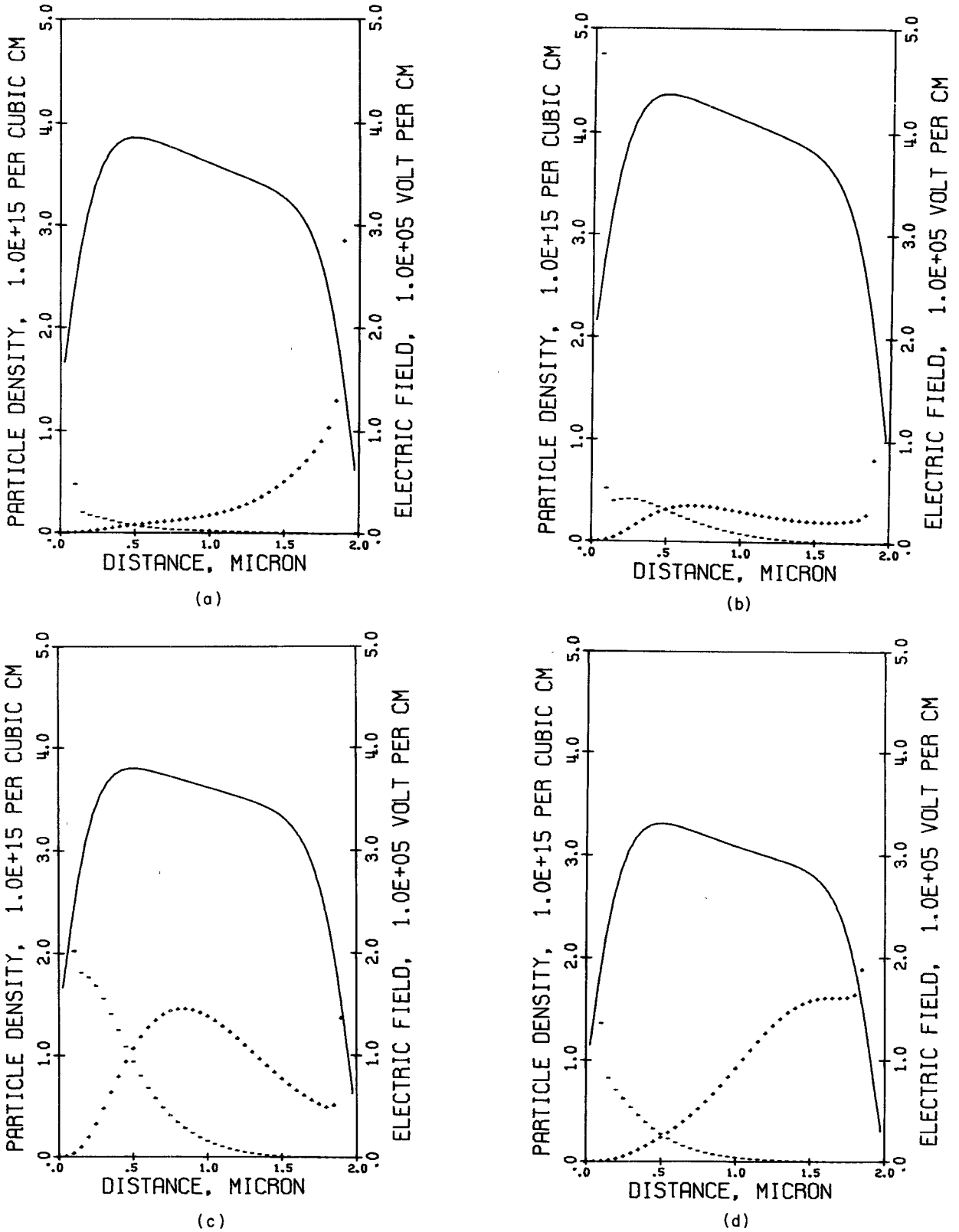

Fig. 10. The electric field (solid line), hole density (plus sign), and electron density (minus sign) versus distance for different values of phase angle in the IMPATT operation for an Si n^+-p-p^+ diode (J_{dc} = 1000 A/cm^2; V_{RF} = 10 V, f = 25 GHz). (a) Phase = 0.00°. (b) Phase = 90.00°. (c) Phase = 180.00°. (d) Phase = 270.00°.

solution for P, N, and E at different phase angles when the preceding simulation becomes periodic.

Simulation of Current-Driven RF Operation

In this case, the total current density across the diode versus time is specified. For the explicit method, the terminal voltage at the $(K+1)$th time step can be calculated from the given total current density by using the following relation:

$$JT^K = \epsilon W_d(VT^{K+1} - VT^K)/\Delta t + JIN^K \qquad (99)$$

where JIN^K is the induced current density at the Kth time step. This calculated VT^{K+1} is used as a boundary condition just as in the voltage-driven case. For the implicit method, the value of $\Delta E_{JW}{}^{K+1}$ can be calculated from

$$\Delta E_{JW}{}^{K+1} = \frac{\Delta JT^{K+(1/2)}}{(\epsilon/\Delta t) + q[(\partial JP/\partial E)_{JW}{}^K + (\partial JN/\partial E)_{JW}{}^K + (\partial JP/\partial P)_{JW}{}^K QEP_{JW,JW} + (\partial JN/\partial N)_{JW}{}^K QEN_{JW,JW}{}^K]}. \qquad (100)$$

The derivation of the preceding equation is similar to that of (97), except that the $\Delta JT^{K+(1/2)}$ is redefined to be the change of total current density between the Kth and $(K+1)$th time step.

The boundary conditions for the particle densities are still identical with those used in the dc static calculation.

Fig. 11 shows a simulation by the explicit method of the TRAPATT mode of operation of the same n^+-p-p^+ Si diode. Before the zero phase angle, the diode is assumed to be biased at a constant current density of 0.1 A/cm², and the values of P, N, and E are calculated by the dc program. Starting from the zero phase angle, the diode is driven by a constant current density of 20 000 A/cm². The simulation is continued until the terminal voltage has recovered to the dc breakdown voltage (this moment is defined to be 180° phase angle). Then the diode is assumed to be driven by the 0.1 A/cm² current density between 180° and 360° phase angle. Fig. 12 shows P, N, and E versus distance at several different phase angles.

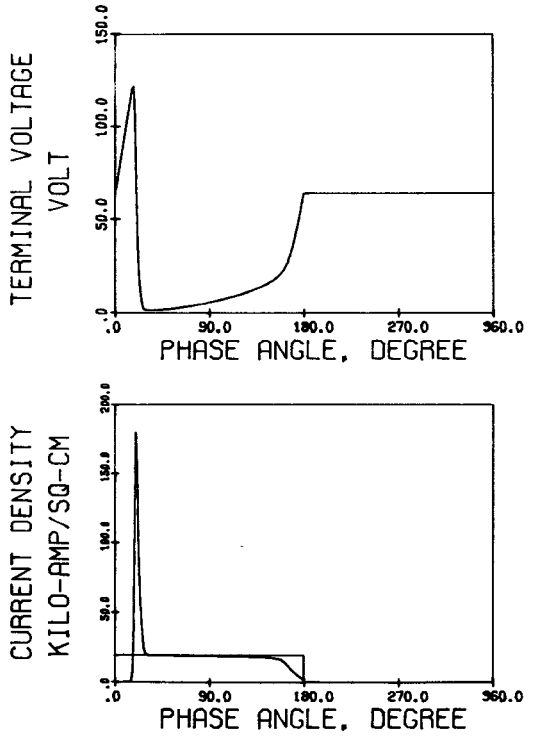

Fig. 11. Terminal voltage, total current, and particle current waveforms for the TRAPATT operation of an Si n^+-p-p^+ diode (diode width = 2 μm; f = 3.0 GHz; JTO = 0.1 A/cm²; JT = 20 kA/cm²).

Simulation of Circuit-Loaded Devices

The objective of this kind of simulation is to investigate the behavior of the device when it is connected to a microwave circuit with some kind of dc bias source. There are basically two different approaches. One is the approach used by Evans and Scharfetter [39], the other one is the approach of Matsumura and Abe [40].

In the approach of Evans and Scharfetter [39], the circuit is divided into several elements, each one of these elements is represented by its $ABCD$ matrix. The driving point admittance $Y_d(\omega)$ at the device point can be found by repeated multiplication of these matrices. Then the impulse response $y(t)$ of this circuit is obtained from the inverse Fourier transform of the driving point admittance $Y_d(\omega)$, i.e.,

$$y_d(t) = \frac{1}{2\pi}\int_{-\infty}^{\infty} Y_d(\omega)\exp(-j\omega t)\,d\omega. \qquad (101)$$

The transfer admittance $Y_b(\omega)$ and the impulse transfer admittance $y_b(t)$ from the biasing voltage source V_b to the device point can be found in a similar way.

The total current across the device in the frequency domain $JT(\omega)$ is given by

$$JT(\omega) = -Y_d(\omega)\cdot V_{RF}(\omega) + Y_b(\omega)\cdot V_b. \qquad (102)$$

At any instant of time t, the total current across the device in the time domain $JT(t)$ is given by the convolution of the impulse admittance and the voltage:

$$JT(t) = Y_b(0)\cdot V_b - \int_{t-T}^{t} y_d(t-\tau)\cdot V_{RF}(\tau)\,d\tau. \qquad (103)$$

The convolution is truncated at T, beyond which y_d is negligibly small. The calculation of $JT(t)$ has to be done at each time step, and is used as the boundary condition for the electric field in the implicit method. For the explicit method, the terminal voltage $VT(t)$ can be calculated similarly using the impulse impedance. The boundary conditions for the particle densities are still the same as those in the dc static calculation.

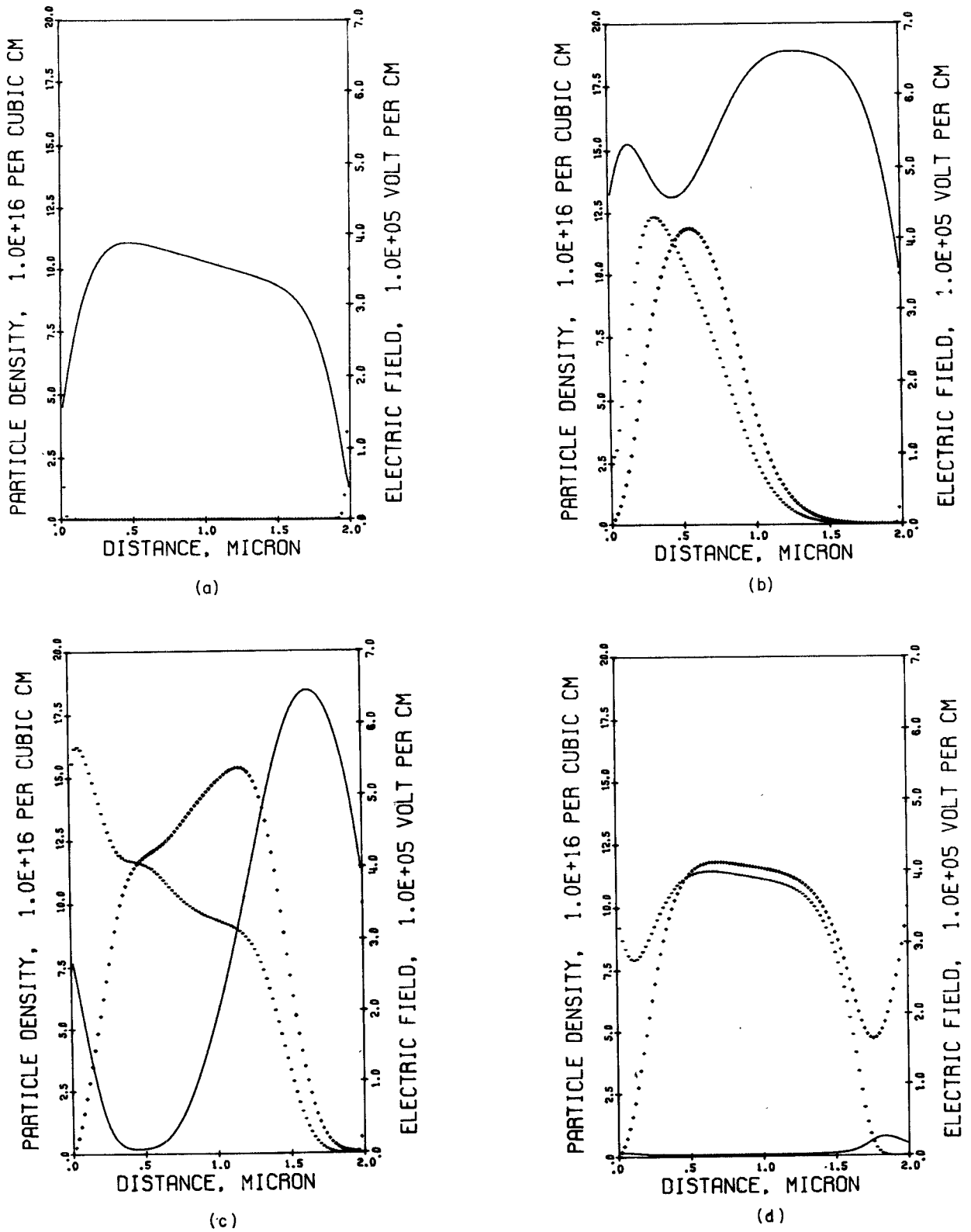

Fig. 12. The electric field (solid line), hole density (plus sign), and electron density (minus sign) versus distance for different values of phase angle in the TRAPATT operation for the Si n^+-p-p^+ diode. (a) Phase = 0.00°. (b) Phase = 18.43°. (c) Phase = 20.60°. (d) Phase = 29.28°. (e) Phase = 118.19°. (f) Phase = 172.41°.

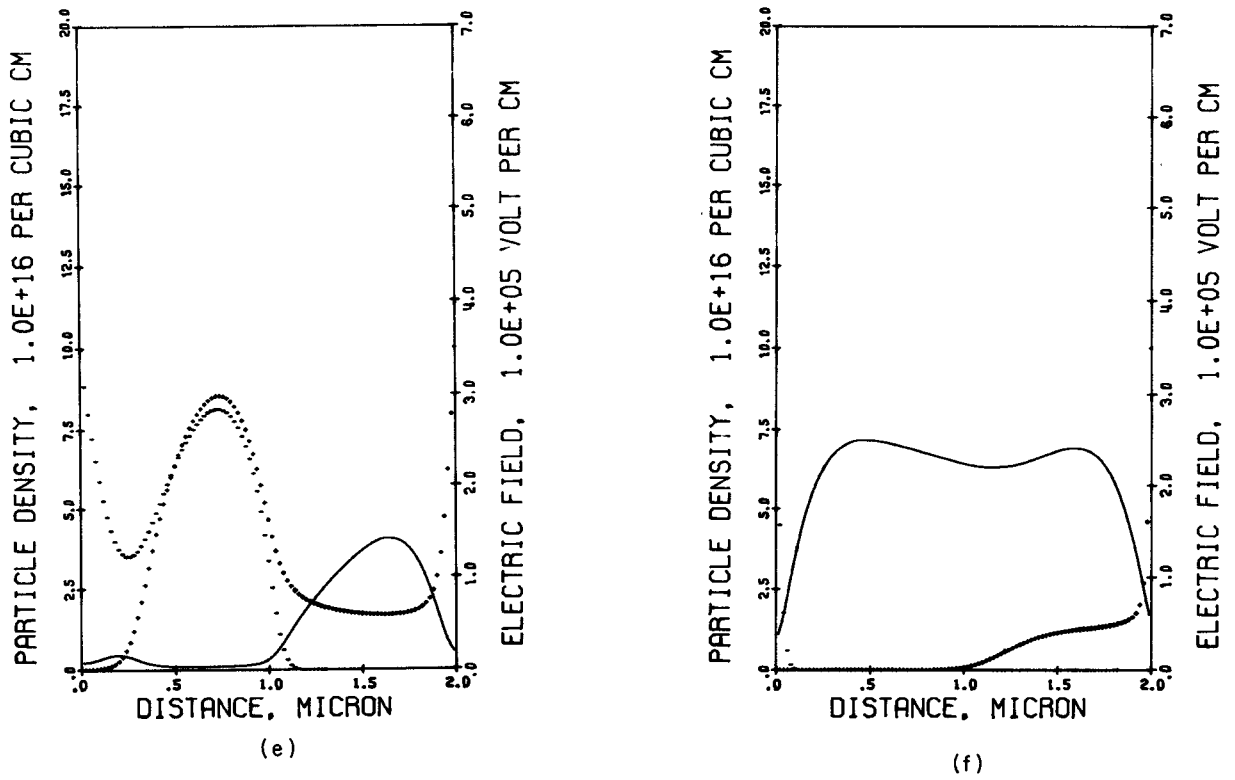

Fig. 12. (*Continued.*)

In the approach of Matsumura and Abe [40], the device is assumed to be connected to a transmission line filled with several tuning slugs and terminated with a loading resistor in series with a biasing voltage source as shown in Fig. 13. The characteristic impedances of the transmission line and tuning slugs are assumed to be independent of frequency. In the transmission line, there is a forward voltage wave $v^+(x,t)$ and a forward current wave $i^+(x,t)$ that travel toward the load, and a backward voltage wave $v^-(x,t)$ and a backward current wave $i^-(x,t)$ that travel toward the device. These traveling waves do not change their shapes until they reach a discontinuity. Hence, in the uniform portion of the transmission line, for each Δt advancement these waves change as follows:

$$v^+(x + \Delta x, t + \Delta t) = v^+(x,t) \tag{104}$$

$$v^-(x - \Delta x, t + \Delta t) = v^-(x,t) \tag{105}$$

$$i^+(x,t) \equiv v^+(x,t)/Z_0 \tag{106}$$

and

$$i^-(x,t) \equiv -v^-(x,t)/Z_0 \tag{107}$$

where Z_0 is the characteristic impedance of the transmission line and $\Delta x/\Delta t = c$ (wave velocity).

At the discontinuity (for example, at x_1 in Fig. 13) given $v^+(x_1 - \Delta x,t)$ and $v^-(x_1 + \Delta x,t)$, $v^+(x_1,t + \Delta t)$ and $v^-(x_1,t + \Delta t)$ can be calculated from

$$v^+(x_1,t + \Delta t) = v^-(x_1 + \Delta x,t)\frac{Z_0 - Z_1}{Z_1 + Z_0} + v^+(x_1 - \Delta x,t)\frac{2Z_0}{Z_1 + Z_0} \tag{108}$$

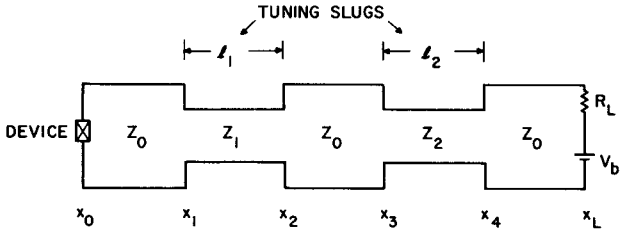

Fig. 13. Circuit model used in the approach of Matsumura and Abe [40].

and

$$v^-(x_1,t + \Delta t) = v^+(x_1 - \Delta x,t)\frac{Z_1 - Z_0}{Z_1 + Z_0} + v^-(x_1 + \Delta x,t)\frac{2Z_1}{Z_1 + Z_0}. \tag{109}$$

At the load plane x_L the following results:

$$v^-(x_L,t + \Delta t) = \frac{V_b/R_L}{(1/Z_0 + 1/R_L)} + v^+(x_L - \Delta x,t)\frac{(1/Z_0 - 1/R_L)}{(1/Z_0 + 1/R_L)}. \tag{110}$$

At the device plane x_0 the following results:

$$VT(t + \Delta t) = VT(t) + \frac{\Delta t \cdot W_d}{\epsilon A_d} \cdot [VT(t) - 2v^-(x_0 + \Delta x,t)/Z_0 - JIN(t) \cdot A_d] \tag{111}$$

where A_d is the device area and $JIN(t)$ is the induced cur-

rent. This calculated VT is then used as the boundary condition for the electric field in the explicit method. For the implicit method, $JT(t + \Delta t)$ can be found in a similar way.

When performing this kind of simulation, the investigator has no prior knowledge about the oscillation frequency and amplitude or the mode of operation in which the device will operate. Hence, although this kind of simulation will yield results that are closer to physical reality, it is very costly for analysis and optimization purposes.

Comparison of The Implicit and Explicit Methods for the Simulation of Avalanche Diodes

Although the explicit method is very inexpensive for each advancement of Δt, because the size of Δt is limited by the stability conditions, it may become expensive when the particle densities are high, the mobilities are high or when the simulation is to be carried over a long time duration. For Si IMPATT devices, the explicit method has definitely proven to be less expensive. On the other hand, for the calculation of the dc solution the explicit method is approximately twice as expensive as the implicit method.

As can be seen, the implicit method is complicated and hence, is more expensive for each Δt. On the other hand, it is more stable numerically and the time step Δt can usually be made very large. Because of this, the implicit method is often used to calculate the dc static solution by setting the time step Δt to be infinite. The stability conditions for the implicit method have not been investigated. It has been observed that if the initial guess is not good, the implicit method sometimes becomes unstable with $\Delta t = \infty$, while the explicit method always converges to a dc static solution even with a poor initial guess, although it may cost more because the calculation must be carried over a large number of time steps. Usually, the explicit method is used to calculate the first set of dc static solutions of a device, then the implicit method is used to find the other dc static solutions for different bias currents using the first set of solutions as initial guesses. For large-signal simulation of Si IMPATT and TRAPATT diodes, the explicit method has always been used by the authors. For the simulation of a transistor, the implicit method is more desirable because a high doping density is involved.

Appendix
The Formulation for the Construction of the Matrix Equation in the Implicit Method

The terms in the matrix equation (50) in the implicit method can be calculated as follows. For each field point I, the following are calculated:

$$KTOQDX = kT/(q\Delta x)$$

$$DUPDE_I = \frac{\partial UP_I}{\partial E_I} \qquad DUNDE_I = \frac{\partial UN_I}{\partial E_I}$$

$$DIPDE_I = \frac{\partial IP_I}{\partial E_I} \qquad DINDE_I = \frac{\partial IN_I}{\partial E_I}.$$

When $E_I \geqq 0$, the following results:

$$\frac{\partial JP_I}{\partial P_J} = (E_I + KTOQDX)\,UP_I \tag{112}$$

$$\frac{\partial JP_I}{\partial P_{J+1}} = -KTOQDX \cdot UP_I \tag{113}$$

$$\frac{\partial JP_I}{\partial N_J} = \frac{\partial JP_I}{\partial N_{J+1}} = 0 \tag{114}$$

$$\frac{\partial JP_I}{\partial E_I} = UP_I \cdot P_J + DUPDE_I \cdot [E_I \cdot P_J - KTOQDX(P_{J+1} - P_J)] \tag{115}$$

$$\frac{\partial JN_I}{\partial N_J} = -KTOQDX \cdot UN_I \tag{116}$$

$$\frac{\partial JN_I}{\partial N_{J+1}} = (E_I + KTOQDX) \cdot UN_I \tag{117}$$

$$\frac{\partial JN_I}{\partial P_J} = \frac{\partial JN_I}{\partial P_{J+1}} = 0 \tag{118}$$

and

$$\frac{\partial JN_I}{\partial E_I} = UN_I \cdot N_{J+1} + DUNDE_I \cdot [E_I \cdot N_{J+1} + KTOQDX \cdot (N_{J+1} - N_J)]. \tag{119}$$

When $E_I < 0$, the following results:

$$\frac{\partial JP_I}{\partial P_J} = KTOQDX \cdot UP_I \tag{120}$$

$$\frac{\partial JP_I}{\partial P_{J+1}} = (E_I - KTOQDX) \cdot UP_I \tag{121}$$

$$\frac{\partial JP_I}{\partial N_J} = \frac{\partial JP_I}{\partial N_{J+1}} = 0 \tag{122}$$

$$\frac{\partial JP_I}{\partial E_I} = UP_I \cdot P_{J+1} + DUPDE_I \cdot [E_I \cdot P_{J+1} - KTOQDX \cdot (P_{J+1} - P_J)] \tag{123}$$

$$\frac{\partial JN_I}{\partial N_J} = (E_I - KTOQDX) \cdot UN_I \tag{124}$$

$$\frac{\partial JN_I}{\partial N_{J+1}} = KTOQDX \cdot UN_I \tag{125}$$

$$\frac{\partial JN_I}{\partial P_J} = \frac{\partial JN_I}{\partial P_{J+1}} = 0 \tag{126}$$

and

$$\frac{\partial JN_I}{\partial E_I} = UN_I \cdot N_J + DUNDE_I \cdot [E_I \cdot N_J + KTOQDX \cdot (N_{J+1} - N_J)]. \tag{127}$$

When sign(x) is defined as follows:

$$\text{sign}\ (x) = \begin{cases} +1, & \text{if } x \geqq 0 \\ -1, & \text{if } x < 0 \end{cases}$$

the generation terms are calculated as

$$\frac{\partial G_I}{\partial P_J} = IP_I \cdot \frac{\partial JP_I}{\partial P_J} \cdot \text{sign}\ (JP_I) \tag{128}$$

$$\frac{\partial G_I}{\partial N_J} = IN_I \cdot \frac{\partial JN_I}{\partial N_J} \cdot \text{sign}\ (JN_I) \tag{129}$$

$$\frac{\partial G_I}{\partial P_{J+1}} = IP_I \cdot \frac{\partial JP_I}{\partial P_{J+1}} \cdot \text{sign}\ (JP_I) \tag{130}$$

$$\frac{\partial G_I}{\partial N_{J+1}} = IN_I \cdot \frac{\partial JN_I}{\partial N_{J+1}} \cdot \text{sign}\ (JN_I) \tag{131}$$

and

$$\frac{\partial G_I}{\partial E_I} = DIPDE_I \cdot |JP_I| + DINDE_I \cdot |JN_I| + IP_I \cdot \frac{\partial JP_I}{\partial E_I} \cdot \text{sign}\ (JP_I) + IN_I \cdot \frac{\partial JN_I}{\partial E_I} \cdot \text{sign}\ (JN_I). \tag{132}$$

Then at each space-charge point J, it can be seen that

$$\frac{\partial G_J}{\partial E_{I-1}} = \frac{1}{2}\frac{\partial G_{I-1}}{\partial E_{I-1}} \tag{133}$$

$$\frac{\partial G_J}{\partial E_I} = \frac{1}{2}\frac{\partial G_I}{\partial E_I} \tag{134}$$

$$\frac{\partial G_J}{\partial P_{J-1}} = \frac{1}{2}\frac{\partial G_{I-1}}{\partial P_{J-1}} \tag{135}$$

$$\frac{\partial G_J}{\partial N_{J-1}} = \frac{1}{2}\frac{\partial G_{I-1}}{\partial N_{J-1}} \tag{136}$$

$$\frac{\partial G_J}{\partial P_J} = \frac{1}{2}\left(\frac{\partial G_{I-1}}{\partial P_J} + \frac{\partial G_I}{\partial P_J}\right) \tag{137}$$

$$\frac{\partial G_J}{\partial N_J} = \frac{1}{2}\left(\frac{\partial G_{I-1}}{\partial N_J} + \frac{\partial G_I}{\partial N_J}\right) \tag{138}$$

$$\frac{\partial G_J}{\partial P_{J+1}} = \frac{1}{2}\frac{\partial G_I}{\partial P_{J+1}} \tag{139}$$

$$\frac{\partial G_J}{\partial N_{J+1}} = \frac{1}{2}\frac{\partial G_I}{\partial N_{J+1}} \tag{140}$$

$$\frac{\partial}{\partial P_{J-1}}\left(\frac{\partial JP}{\partial x}\right)_J = -\frac{1}{\Delta x}\frac{\partial JP_{I-1}}{\partial P_{J-1}} \tag{141}$$

$$\frac{\partial}{\partial N_{J-1}}\left(\frac{\partial JN}{\partial x}\right)_J = -\frac{1}{\Delta x}\frac{\partial JN_{I-1}}{\partial N_{J-1}} \tag{142}$$

$$\frac{\partial}{\partial N_{J-1}}\left(\frac{\partial JP}{\partial x}\right)_J = \frac{\partial}{\partial P_{J-1}}\left(\frac{\partial JN}{\partial x}\right)_J = 0 \tag{143}$$

$$\frac{\partial}{\partial P_J}\left(\frac{\partial JP}{\partial x}\right)_J = \frac{1}{\Delta x} \cdot \left(\frac{\partial JP_I}{\partial P_J} - \frac{\partial JP_{I-1}}{\partial P_J}\right) \tag{144}$$

$$\frac{\partial}{\partial N_J}\left(\frac{\partial JN}{\partial x}\right)_J = \frac{1}{\Delta x} \cdot \left(\frac{\partial JN_I}{\partial N_J} - \frac{\partial JN_{I-1}}{\partial N_J}\right) \tag{145}$$

$$\frac{\partial}{\partial N_J}\left(\frac{\partial JP}{\partial x}\right)_J = \frac{\partial}{\partial P_J}\left(\frac{\partial JN}{\partial x}\right)_J = 0 \tag{146}$$

$$\frac{\partial}{\partial P_{J+1}}\left(\frac{\partial JP}{\partial x}\right)_J = \frac{1}{\Delta x}\frac{\partial JP_I}{\partial P_{J+1}} \tag{147}$$

$$\frac{\partial}{\partial N_{J+1}}\left(\frac{\partial JN}{\partial x}\right)_J = \frac{1}{\Delta x}\frac{\partial JN_I}{\partial N_{J+1}} \tag{148}$$

$$\frac{\partial}{\partial N_{J+1}}\left(\frac{\partial JP}{\partial x}\right)_J = \frac{\partial}{\partial P_{J+1}}\left(\frac{\partial JN}{\partial x}\right)_J = 0 \tag{149}$$

$$\frac{\partial}{\partial E_{I-1}}\left(\frac{\partial JP}{\partial x}\right)_J = -\frac{1}{\Delta x}\frac{\partial JP_{I-1}}{\partial E_{I-1}} \tag{150}$$

$$\frac{\partial}{\partial E_{I-1}}\left(\frac{\partial JN}{\partial x}\right)_J = -\frac{1}{\Delta x}\frac{\partial JN_{I-1}}{\partial E_{I-1}} \tag{151}$$

$$\frac{\partial}{\partial E_I}\left(\frac{\partial JP}{\partial x}\right)_J = \frac{1}{\Delta x}\frac{\partial JP_I}{\partial E_I} \tag{152}$$

and

$$\frac{\partial}{\partial E_I}\left(\frac{\partial JN}{\partial x}\right)_J = \frac{1}{\Delta x}\frac{\partial JN_I}{\partial E_I}. \tag{153}$$

Finally,

$$-\frac{\partial FP_J}{\partial P_{J-1}} = \frac{\partial}{\partial P_{J-1}}\left(\frac{\partial JP}{\partial x}\right)_J - \frac{\partial G_J}{\partial P_{J-1}} \tag{154}$$

$$-\frac{\partial FP_J}{\partial N_{J-1}} = -\frac{\partial G_J}{\partial N_{J-1}} \tag{155}$$

$$-\frac{\partial FN_J}{\partial P_{J-1}} = -\frac{\partial G_J}{\partial P_{J-1}} \tag{156}$$

$$-\frac{\partial FN_J}{\partial N_{J-1}} = -\frac{\partial}{\partial N_{J-1}}\left(\frac{\partial JN}{\partial x}\right)_J - \frac{\partial G_J}{\partial N_{J-1}} \tag{157}$$

$$\frac{2}{\Delta t} - \frac{\partial FP_J}{\partial P_J} = \frac{2}{\Delta t} + \frac{\partial}{\partial P_J}\left(\frac{\partial JP}{\partial x}\right)_J - \frac{\partial G_J}{\partial P_J} \tag{158}$$

$$-\frac{\partial FP_J}{\partial N_J} = -\frac{\partial G_J}{\partial N_J} \tag{159}$$

$$-\frac{\partial FN_J}{\partial P_J} = -\frac{\partial G_J}{\partial P_J} \tag{160}$$

$$\frac{2}{\Delta t} - \frac{\partial FN_J}{\partial N_J} = \frac{2}{\Delta t} - \frac{\partial}{\partial N_J}\left(\frac{\partial JN}{\partial x}\right)_J - \frac{\partial G_J}{\partial N_J} \tag{161}$$

$$-\frac{\partial FP_J}{\partial P_{J+1}} = \frac{\partial}{\partial P_{J+1}}\left(\frac{\partial JP}{\partial x}\right)_J - \frac{\partial G_J}{\partial P_{J+1}} \tag{162}$$

$$-\frac{\partial FP_J}{\partial N_{J+1}} = -\frac{\partial G_J}{\partial N_{J+1}} \tag{163}$$

$$-\frac{\partial FN_J}{\partial P_{J+1}} = -\frac{\partial G_J}{\partial P_{J+1}} \tag{164}$$

$$-\frac{\partial FN_J}{\partial N_{J+1}} = -\frac{\partial}{\partial N_{J+1}}\left(\frac{\partial JN}{\partial x}\right)_J - \frac{\partial G_J}{\partial N_{J+1}} \tag{165}$$

$$-\frac{\partial FP_J}{\partial E_{I-1}} = \frac{\partial}{\partial E_{I-1}}\left(\frac{\partial JP}{\partial x}\right)_J - \frac{\partial G_J}{\partial E_{I-1}} \tag{166}$$

$$-\frac{\partial FN_J}{\partial E_{I-1}} = -\frac{\partial}{\partial E_{I-1}}\left(\frac{\partial JN}{\partial x}\right)_J - \frac{\partial G_J}{\partial E_{I-1}} \tag{167}$$

$$-\frac{\partial FP_J}{\partial E_I} = \frac{\partial}{\partial E_I}\left(\frac{\partial JP}{\partial x}\right)_J - \frac{\partial G_J}{\partial E_I} \tag{168}$$

$$-\frac{\partial FN_J}{\partial E_I} = -\frac{\partial}{\partial E_I}\left(\frac{\partial JN}{\partial x}\right)_J - \frac{\partial G_J}{\partial E_I} \tag{169}$$

$$FP_J = G_J - \left(\frac{\partial JP}{\partial x}\right)_J \tag{170}$$

and

$$FN_J = G_J + \left(\frac{\partial JN}{\partial x}\right)_J. \tag{171}$$

References

[1] H. K. Gummel, "A self-consistent iterative scheme for one-dimensional steady state transistor calculations," *IEEE Trans. Electron Devices*, vol. ED-11, pp. 455–465, Oct. 1964.

[2] R. W. Hockney, "A fast direct solution of Poisson's equation using Fourier analysis," *J. Ass. Comput. Mach.*, vol. 12, pp. 95–113, 1965.

[3] E. R. Berman and A. L. Ward, "Fortran IV program for gas tubes and other dielectrics," Harry Diamond Lab., Rep. TR-1310, Nov. 5, 1965.

[4] H. N. Gosh, P. H. de la Moneda, and N. R. Dono, "Computer aided transistor design characterization and optimization," *Solid-State Electron.*, vol. 10, pp. 705–726, 1967.

[5] D. M. Caughey, "The computer simulation of gigahertz transistors," presented at the IEEE Int. Electron. Conf., Toronto, Ont., Canada, 1967.

[6] T. W. Collins, "Two-dimensional numerical analysis of integrated bipolar transistors," presented at the Int. Electron Devices Meeting, Washington, D. C., 1968.

[7] J. W. Slotboom, "An accurate numerical one-dimensional solution of the p-n junction under arbitrary transient conditions," *Solid-State Electron.*, vol. 11, pp. 1021–1053, 1968.

[8] A. de Mari, "An accurate numerical steady-state one dimensional solution of the p-n junction," *Solid-State Electron.*, vol. 11, pp. 35–58, 1968.

[9] H. L. Stone, "Iterative solution of implicit approximations of multidimensional partial differential equations," *SIAM J. Numer. Anal.*, vol. 5, pp. 530–558, Sept. 1968.

[10] J. L. Scales and A. L. Ward, "Computer studies of Gunn oscillations in gallium arsenide," Harry Diamond Lab., Rep. TR-1403, Aug. 1968.

[11] D. L. Scharfetter and H. K. Gummel, "Large-signal analysis of a silicon Read diode oscillator," *IEEE Trans. Electron Devices*, vol. ED-16, pp. 64–77, Jan. 1969.

[12] H. K. Gummel, "Computer device modeling," presented at the European Sem. Develop. Res. Conf., Munich, Germany, 1969.

[13] P. U. Calzolari and S. Graffii, "Two-dimensional theory of the uniform base transistor at any injection level," *Alta Freq.*, vol. 38, pp. 126–134, Feb. 1969.

[14] J. W. Slotboom, "Simulation of UHF transistor small signal behavior to 10 GHz for circuit modeling," in *Proc. Cornell Conf. Computerized Electron.*, pp. 369–379, Aug. 1969.

[15] D. P. Kennedy and R. R. O'Brien, "Two-dimensional mathematical analysis of a planar type junction field effect transistor," *IBM J. Res. Develop.*, vol. 13, pp. 662–674, Nov. 1969.

[16] V. Arandjelovic, "General iterative scheme for one dimensional calculations of steady-state electrical properties of transistors," *Int. J. Electron.*, vol. 27, pp. 459–478, 1969.

[17] J. W. Slotboom, "Iterative scheme for 1- and 2-dimensional dc-transistor simulation," *Electron. Lett.*, vol. 5, pp. 677–678, Dec. 1969.

[18] P. Dubock, "D.c. numerical model for arbitrarily biased bipolar transistors in two dimensions," *Electron. Lett.*, vol. 6, pp. 53-55, Feb. 5, 1970.

[19] J. W. Slotboom, "Accurate numerical steady-state solutions for a diffused one-dimensional junction diode," *Solid-State Electron.*, vol. 13, pp. 865–971, 1970.

[20] ——, "Computer-aided two dimensional analysis of the junction field-effect transistor." *IBM J. Res. Develop.*, vol. 14, pp. 95–116, Mar. 1970.

[21] M. Kurata, "Steady-state transistor calculations for higher collector voltages," *Proc. IEEE* (Lett.), vol. 58, pp. 485–487, Mar. 1970.

[22] B. V. Gokhale, "Numerical solutions for a one-dimensional silicon n-p-n transistor," *IEEE Trans. Electron Devices*, vol. ED-17, pp. 594–602, Aug. 1970.

[23] V. Arandjelovic, "Accurate numerical steady-state solutions for a diffused one-dimensional junction diode," *Solid-State Electron.*, vol. 13, pp. 865–871, 1970.

[24] M. Matsumura, "Bias field distribution of high power p-n-n^+ IMPATT diodes," *Trans. IECE (Japan)*, vol. 53-C, pp. 88–95, Feb. 1970.

[25] P. T. Greiling, "Large-signal characteristics of avalanche-diode oscillators," Ph.D. dissertation, Univ. Michigan, Ann Arbor, June 1970.

[26] D. van Dorpe and N. H. Xuong, "Mathematical 2-dimensional model of semiconductor devices," *Electron. Lett.*, vol. 7, pp. 47–50, Jan. 1971.

[27] S. P. Yu, W. Tantraporn, and J. D. Young, "Transit-time negative conductance in GaAs bulk-effect diodes," *IEEE Trans. Electron Devices*, vol. ED-18, pp. 88–93, Feb. 1971.

[28] M. Kurata, "A small-signal calculation for one-dimensional transistors," *IEEE Trans. Electron Devices*, vol. ED-18, pp. 200–210, Mar. 1971.

[29] J. A. Kilpatrick and W. D. Ryan, "Two-dimensional analysis of lateral-base transistors," *Electron. Lett.*, vol. 7, pp. 226–227, May 1971.

[30] M. Reiser, "Difference methods for the solution of the time-dependent semiconductor flow equations," *Electron. Lett.*, vol. 7, pp. 353–355, June 1971.

[31] S. C. Choo, "Numerical analysis of a forward-biased step-junction P-L-N diode," *IEEE Trans. Electron Devices*, vol. ED-18, pp. 574–586, Aug. 1971.

[32] D. P. Kennedy and R. R. O'Brien, "Two-dimensional analysis of J.F.E.T. structures containing a low-conductivity substrate," *Electron. Lett.*, vol. 7, pp. 714–716, Dec. 1971.

[33] G. D. Hachtel, R. C. Joy, and J. W. Cooley, "A new efficient one-dimensional analysis program for junction device modeling," *Proc. IEEE (Special Issue on Computers in Design)*, vol. 60, pp. 86–98, Jan. 1972.

[34] J. A. G. Slatter, "Fundamental modeling of cylindrical geometry bipolar transistors," *Electron. Lett.*, vol. 8, pp. 222–223, May 1972.

[35] T. I. Seidman and S. C. Choo, "Iterative scheme for computer simulation of semiconductor devices," *Solid-State Electron.*, vol. 15, pp. 1229–1235, 1972.

[36] D. van Dorpe, J. Borel, G. Merckel, and P. Saintot, "An accurate two-dimensional numerical analysis of the MOS transistor," *Solid-State Electron.*, vol. 15, pp. 547–557, 1972.

[37] H. H. Heimeier, "A two-dimensional numerical analysis of a silicon N-P-N transistor," *IEEE Trans. Electron Devices*, vol. ED-20, pp. 708–714, Aug. 1973.

[38] J. W. Slotboom, "Computer-aided two-dimensional analysis of bipolar transistors," *IEEE Trans. Electron Devices*, vol. ED-20, pp. 669–679, Aug. 1973.

[39] W. J. Evans and D. L. Scharfetter, "Characteristics of avalanche diode TRAPATT oscillators," *IEEE Trans. Electron Devices*, vol. ED-17, pp. 397–404, May 1970.

[40] M. Matsumura and H. Abe, "Computer simulation of anomalous-mode oscillation in silicon avalanche diodes," *IEEE Trans. Microwave Theory Tech.* (Corresp.), vol. MTT-18, pp. 975–977, Nov. 1970.